

Evaluation of Image Compression Methods for used in Wireless Multimedia Sensor Networks

H.Benabbes, Kh.Benahmed, M.Beladgham and B.Draoui,

Laboratory of Energetic in Arid Zones, Tahri
Mohammed University Bechar, Street independence bp 417 Bechar, Algeria

Abstract

In Wireless Multimedia Sensor Networks (WMSN) the large size of multimedia data such as image requires finding optimal solutions. To solve the problems of energy consumption and bandwidth during processing and transmission, there are solutions that address these problems, such as image compression. Currently, the most effective methods are based on the wavelet transform, which allows spatially decorrelating the image i.e., it is necessary to develop progressive coders interested in the content of the image before compression. Several researchers in this axis show that SPHIT is the best choice for low energy compression algorithms because of its ability to provide higher compression ratio with low complexity and better image quality, but what is the best transform used by SPHIT? Knowing that there are several wavelet transforms. This work deals with four compression methods applied to color images. The proposed method is based on the lifting scheme coupled with the SPIHT coding and wavelets biorthogonal Cohen-Daubechies-Feauveau wavelet (CDF 9/7). This method is compared with three methods: lifting scheme coupled with the SPIHT coding and wavelets biorthogonal Gall 5/3, CDF 9/7 (Filter Bank) coupled with the SPIHT and CDF 9/7 (Lifting scheme) coupled with the Embedded Zerotrees of Wavelet transforms (EZW) coding based on the following evaluations factors: image quality (Peak Signal-to-Noise Ratio (PSNR), Mean Square Error (MSE), Structural Similarity Index (MSSIM) and Fidelity Information Visual (FIV)) and energy consumption (Compression Ratio (CR)).

Keywords

Compression, Wireless Multimedia Sensor Networks, energy consumption, SPIHT, lifting, DWT

1. Introduction

Because of the astonishing speed of technology developments, particularly in the field of semiconductors manufacture, electronic equipment has become smaller and cheaper. The field of sensor networks Wireless Multimedia (WMSN) is among the areas that have benefited most from these developments. A multimedia sensor node has a number of characteristics such as limited energy resources. The nature and the specification of the multimedia data, such that image, causes problems in a sensor node in the processing and transmission of data. An image contains a plurality of pixels correlated with each other. However, because of this correlation; data contain a large amount of redundancy that occupies large storage space and reduces

bandwidth. There are three types of data redundancy; spatial redundancy, temporal redundancy and spectral redundancy. The main purpose of compression is to reduce the size of data for storage and transmitting them in a minimum bandwidth, while maintaining acceptable visual quality of the reconstructed image. Compression must also ensure a certain period of network life. Several researchers [1-5] have shown that SPHIT encoder is the best choice for low power consumption compression algorithms because of its ability to provide higher compression ratio (CR) with low complexity and better image quality (PSNR, MSE).

2. Compression and Reconstruction image in WMSN

Data compression can be performed with lossy or without loss. Lossy compression is often preferred for low speed transmissions (e.g image transmission); it loses detail in the image while remaining within acceptable limits. Compressing image in WMSN is generally as indicated in Figure 1.

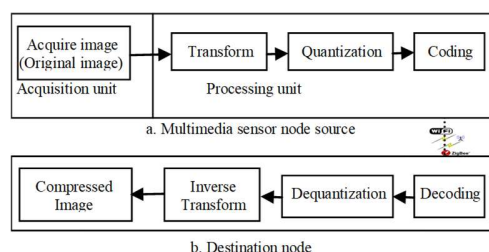


Figure 1. Diagram compression / transmission and decompression of image

In Figure 1.a, First original digital image (acquired image) is usually transformed into another field, where it is strongly-correlated using a transformation. This decorrelation concentrates the important image information in a more compact form. The compressor then removes redundancy in the transformed image and stores it in a file or stream of compressed data. In the second step, the quantization block reduces the accuracy of the output signal converted in accordance with predetermined fidelity criteria.

Also this step reduces the psycho-visual redundancy of the input image. Quantization operation is a reversible process and can be omitted when there is need of compression without error or loss. In the last step of data compression model the encoder symbol creates a fixed or variable length code to represent the output quantification and maps the output in accordance with the code. A variable length code is commonly used to represent the set of mapped and quantified data. It assigns short code words to common output values and reduces the coding redundancy.

According to the coding, it means the bit stream sending a multimedia sensor node source to another destination node via Wifi, Zigbee or other communication techniques. On the other hand (destination node), a reversible operation i.e, the reverse decompression compression processing produce the recovered image as shown in Figure 1.b.

3. Biorthogonal 9/7 Wavelet Transform

The CDF 9/7 wavelet transform belongs to the family of symmetric biorthogonal wavelets [6-9]. The low-pass filters associated with the wavelet to obtain the approximation coefficients are given as follows $p = 9$ coefficients for the analysis, $p = 7$ coefficients in the synthesis are described in Table I.

TABLE I THE ANALYSIS FILTER COEFFICIENTS

i	Analysis filter coefficients	
	Low-pass filter	High-Pass Filter
0	0,602949018236000	0,557543526229000
1	0,266864118443000	-0,295635881557000
2	-0,0782232665290000	-0,0287717631140000
3	-0,0168641184430000	0,0456358815570000
4	0,0267487574110000	

The CDF 9/7 wavelet transform has a large number of vanishing moments ($N = 4$) for a relatively short support. This feature plays an important role in image compression [10, 11]. The following figure shows the representation of the wavelet CDF 9/7.

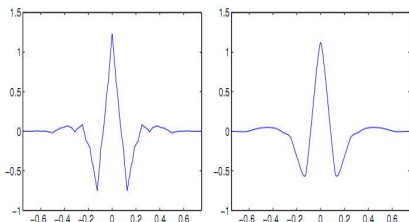


Figure 2. CDF 9/7 wavelet ψ and $\tilde{\psi}$

In this work, we introduced the lifting structure in

the CDF 9/7 wavelet transform. This algorithm is characterized by its effectiveness in the memory space used for the transform coefficients. The lifting scheme consists of two phases: one for analysis or decomposition, and the other for synthesis or reconstruction, and each phase consist of three steps of splitting, prediction and updating. The decomposition phase consists of three steps: split, predict and update see (Figure 3.).

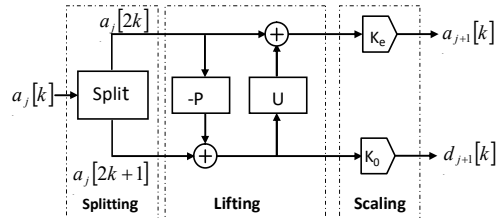


Figure 3. Lifting analysis structure

The CDF 9/7 wavelet of lifting structure is composed of four floors: two predictions operators and two update operators.

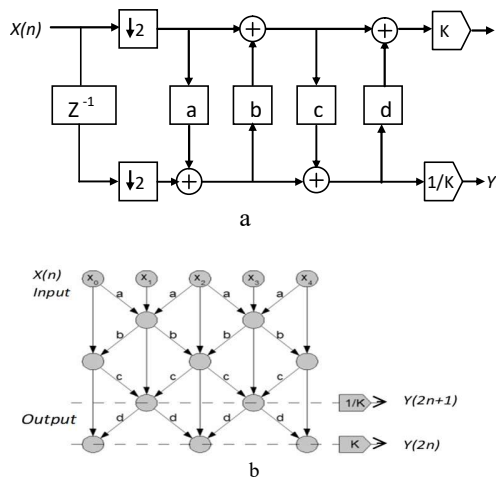


Figure 4. Split, Predict and Update Steps of forward CDF 9/7 wavelet using Lifting scheme; (a) Lifting implementation of the analysis side of the CDF 9/7 filter bank; (b) Structure of the CDF 9/7 filter.

The following equation describes the four stages of "lifting" and the two steps "Scaling".

$$\begin{cases} Y(2n+1) \leftarrow X(2n+1) + (a \times [X(2n) + X(2n+2)]), \\ Y(2n) \leftarrow X(2n) + (b \times [Y(2n-1) + Y(2n+1)]), \\ Y(2n+1) \leftarrow Y(2n+1) + (c \times [Y(2n) + Y(2n+2)]), \\ Y(2n) \leftarrow Y(2n) + (d \times [Y(2n-1) + Y(2n+1)]), \end{cases} \quad (1)$$

$$\begin{cases} Y(2n+1) \leftarrow -K \times Y(2n+1), \\ Y(2n) \leftarrow \left(\frac{1}{K}\right) \times Y(2n), \end{cases} \quad (2)$$

When parameter values are:

$$\begin{aligned}
 a &= -1.149604398 \\
 b &= -0.4435068522 \\
 c &= 0.8829110762 \\
 d &= 0.0529801185 \\
 K &= 1.586134342
 \end{aligned}$$

4. SPIHT Coding Scheme

When decomposition of the image is obtained, we try to find a way to encode the wavelet coefficients in an effective result, taking redundancy and storage space into consideration SPIHT. [14] This coding scheme deserves special attention because it provides the following, good high PSNR, image quality, especially for colour images; it is optimized for progressive image transmission; produces a fully embedded coded file; has a simple quantization algorithm; has fast coding/decoding (almost symmetric); has wide applications, is completely adaptive; can code to exact bit rate or distortion and is efficient combination with error protection.

This technique takes into account the limits between the coefficients across subbands at different levels [10]. [15] The first is always the same: if there is a coefficient at the highest level of processing in a particular sub-band considered insignificant against a particular threshold, it is very likely that his descendants in the lower levels are too insignificant. We can encode a large group of coefficients with every symbol. Figure 5 shows how a spatial orientation tree is defined in a pyramid constructed with four recursive subband splitting. The coefficients are prioritized hierarchically. According to this relationship, the SPIHT algorithm records many bits that specify insignificant coefficients [12-13].

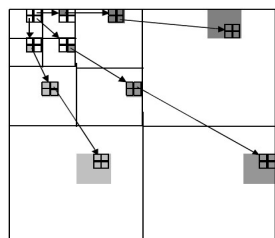


Figure 5. Hierarchical trees in multi-level decomposition

The flowchart of SPIHT is presented in Figure 6. At first, the original image is decomposed into ten sub-bands. Next, the method depicts the maximum number of iterations. Second, the method puts the DWT coefficients into a sorting pass that finds the average of coefficients in all coefficients and encodes the sign of the coefficients significance. Third, the coefficients can be found in the significance of sorting pass which are put in the refinement pass using two bits to require the value of rebuilding in order the true value. The first, second and third steps are iterative and iteration decreases until it reaches the threshold ($T_n = T_{n-1}/2$) and the reconstruction value

($R_n = R_{n-1}/2$). Fourth step, the coding bit access entropy encoding and is then transmitted [24]. The result is in the form of a bitstream.

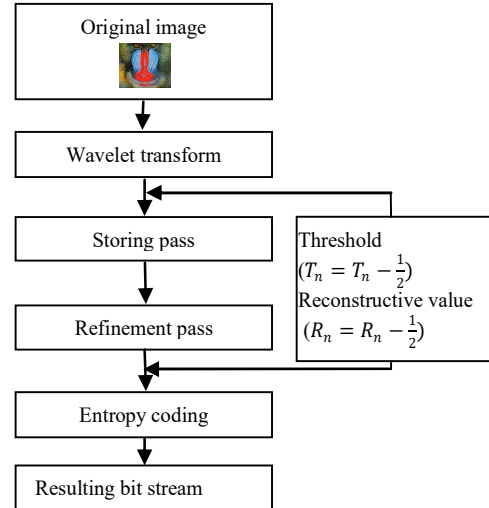


Figure 6. Flowchart of SPIHT.

5. Algorithm

Before applying biorthogonal CDF9/7 based on Lifting scheme on the color image, the RGB color images are converted into YCbCr form, and then applying Wavelet transform on each layer independently, this means each layer from YCbCr are compressed as a grayscale image. YCbCr refers to the color resolution of digital component video signals, which is based on sampling rates. In order to compress bandwidth, Cb and Cr are sampled at a lower rate than Y, which is technically known as "chroma subsampling." This means that some color information in the image is being discarded, but not brightness (luma) information. We obtain the best rate of compression using the rich less layer for the chromatic component Cb and Cr.

$$\begin{cases} Y = 0.2989 * R + 0.5866 * G + 0.1145 * B \\ Cb = -0.1687 * R - 0.3312 * G + 0.5 * B \\ Cr = 0.5 * R - 0.4183 * G - 0.0816 * B \end{cases} \quad (3)$$

When the decomposition image is obtained, we try to find a way to code the Wavelet transform into an efficient result, taking redundancy and storage space into consideration. After, we apply SPIHT algorithm on each layer (Y,Cr,Cb) independently .

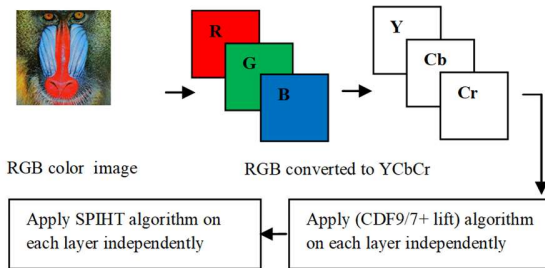


Figure 5. Complete steps image compression technique using Wavelet transform (DWT) coupled with SPIHT

This process is repeated for every resolution in the case of level 3 decompositions. The encoding / decoding can be terminated at any time, with the best reproduction obtained up to that point. This is made possible because of the progressive nature of the coding algorithm.

6. Image compression performance criteria

Energy consumption, for a multimedia sensor is decreases measured by the *compression ratio* (Cr) as shown in formula (3); when the compression ratio is higher, energy consumption is less.

$$Cr = \frac{Bo}{Bi} \quad (4)$$

Where Bo , is the output compressed sequence length, Bi is the uncompressed input length. Objective measurements are based on mathematical criteria for evaluating image quality. The main quality criteria used to measure the performance of optical instruments [14] are:

The *Mean Square Error (MSE)*, the simplest setting of the image quality measure is the MSE. The great value of MSE means that the image quality is poor. The MSE is defined as follows:

$$MSE = \frac{1}{M \cdot N} \cdot \sum_{i=0}^{M-1} \sum_{j=0}^{N-1} [I(i, j) - \hat{I}(i, j)]^2 \quad (5)$$

With: $I(i, j)$ represents the original image, $\hat{I}(i, j)$ is the degraded image. M and N are the number of rows and columns.

Peak Signal-to-Noise Ratio (PSNR), the low value of PSNR means that the image quality is poor. PSNR is defined as follows:

$$PSNR = 10 \log_{10} \left(\frac{(\text{Dynamics of image})^2}{MSE} \right) \quad (6)$$

The Structural Similarity Index (SSIM), Measuring PSNR gives a numerical value for the deterioration, but

nothing about the type of degradation. In addition, as is often noted in [16,17], it does not fully represent the quality perceived by human observers. The similarity compares the brightness, contrast, and structure between each pair of vectors, where the index of structural similarity (SSIM) between two signals x and y is given by the following expression [18,19]:

$$SSIM(x, y) = l(x, y) \cdot c(x, y) \cdot s(x, y) . \quad (7)$$

The formula for the comparison of the brightness is determined as follows:

$$l(x, y) = \frac{2\mu_x\mu_y + C_1}{\mu_x + \mu_y + C_1} , \quad (8)$$

With the average intensity of the signal x is given by:

$$\mu_x = \frac{1}{N} \sum_{i=1}^N x_i , C_1 = (K_1 L)^2 , \quad (9)$$

The constant $K_1 \ll 1$, and L is the dynamic line of pixel values. The contrast comparison expression takes the following form:

$$c(x, y) = \frac{2\sigma_x\sigma_y}{\sigma_x^2 + \sigma_y^2 + C_2} , \quad (10)$$

With $\sigma_x = \sqrt{\mu_x(x^2) - \mu_x^2}$ is the standard deviation of the original signal x , $C_2 = (K_2 L)^2$, and the $K_2 \ll 1$.

The structure of the comparison expression is defined as follows:

$$s(x, y) = \frac{\sigma_{xy} + C_3}{\sigma_x\sigma_y + C_3} = \frac{cov(x, y) + C_3}{\sigma_x\sigma_y + C_3} . \quad (11)$$

Where, $cov(x, y) = \mu_{xy} - \mu_x\mu_y$, and $C_3 = \frac{C_2}{2}$.

Finally, the quality measurement can provide a map of the quality of the local image, which provides more information about the degradation of image quality.

For application, we need a single overall measure of the overall quality of the image that is given by the following formula:

$$MSSIM(I, \hat{I}) = \frac{1}{M} \sum_{i=1}^M SSIM(I, \hat{I}) . \quad (12)$$

Where I and \hat{I} are the reference and degraded images, respectively, I_i and \hat{I}_i are the contents of the images to the local window i . M is the total number of local windows in the image. The *MSSIM* values show greater consistency with the visual quality.

Fidelity Information Visual (VIF), The VIF parameter quantifies Shannon's information that is shared between the reference and distorted images compared to the information contained in the reference image itself. The VIF [21] uses the Gaussian scale mixture model (GSM) in the wavelet

domain. FIV first performs a wavelet decomposition of the image, the wavelet coefficients of each sub-band are modelled as follows: $C = S \cdot U$, where S is a random field (RF) positive multiplier which controls the variations of local coefficients and U is a Gaussian vector (RF) of zero mean and variance σ^2 . The distortion model is $D = GC + V$, where G is a scalar field and gain V is additive Gaussian noise (RF). The FIV is assumed that the distorted images and the pass source through the human visual system HVS whose uncertainty is modelled as a visual noise: N and N' are the source and the distorted image, respectively, where N and N' are average uncorrelated zero. It then calculates $E = C + N$, and $F = D + N'$. The FIV test is then evaluated as [20-23]:

$$FIV = \frac{\sum_{j=1}^M I(C^j; F^j/S^j)}{\sum_{j=1}^M I(C^j; E^j/S^j)} \quad (13)$$

Where $I(X; Y/Z)$ is the conditional mutual information between X and Y , conditioned to Z ; S^j is a realization of S^j for a particular image, the index j runs through all sub-bands in the distorted image. The results of this measurement can be between 0 and 1, where 1 means perfect quality and close to 0 means poor quality.

7. Experimental Results and Discussion

We are interested in lossy compression methods especially Transform-based techniques because their properties are interesting. The 2D wavelets transform combines good spatial and frequency locations [4]. As we work on color image, spatial location and frequency are important.

We applied the proposed algorithm on three test images, shown in figure 7 a. 'monkey', b. 'Lena' and c. 'satellite image' of sizes 512x512 encoded by 8bpp.

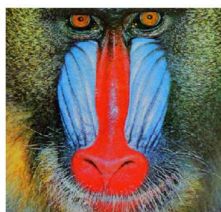


Figure. 7. Test images - Original images

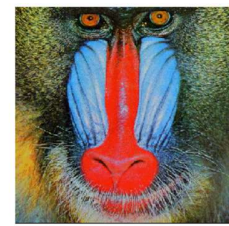
The importance of our work lies in the possibility of increasing the compression ratio for which the image quality is acceptable. The estimates and judgments of the compressed image quality are given by the compression ratio (Cr), MSE, PSNR, the index of similarity MSSIM and VIF. Figure 8 below illustrates the compressed image quality for different bit-rate values (number of bits per pixel).



Bit Rate (bpp)=0.125
CR = 98.44%



Bit Rate (bpp)=0.75
CR = 90.63%



Bit Rate (bpp)=2
CR = 75.00%



Bit Rate (bpp)=0.125
CR = 98.44%



Bit Rate (bpp)=0.75
CR = 90.63%



Bit Rate (bpp)=2
CR = 75.00%



Bit Rate (bpp)=0.125
CR = 98.44%



Bit Rate (bpp)=0.75
CR = 90.63%

Bit Rate (bpp)=2
CR = 75%

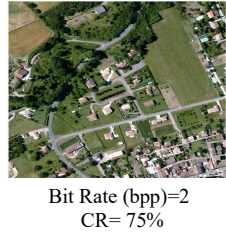


Figure 8. 'Monkey', 'Lena' and 'Concord aerial' images compressed with CDF9/7 (Lifting scheme) and SPIHT coding.

To show the performance of the proposed method, we will now make a comparison between these different types of processing (CDF 9/7 (Filter Bank); Gall 5/3 (lift system) and CDF 9/7 (lifting speed) coupled with coding SPIHT and CDF 9/7 (lifting system) combined with EZW coding. For each application, we vary the bit rate of 0.125 to 2, and we calculate the CR, PSNR, MSSIM and FIV. The results obtained are given in the table II.

TABLE I. CR, MSE, PSNR, SSIM AND VIF VARIATION USING DIFFERENT METHODS FOR THE MONKEY, LENA AND CONCORD AERIAL IMAGES.

Image	Bit Rate (bpp)	CDF9/7 (Lifting) + SPIHT					Gall5/3 (Lifting) + SPIHT					CDF9/7(Filter bank) + SPIHT					CDF9/7 (Lifting)+ EZW				
		CR	MSE	PSNR	MSSIM	VIF	CR	MSE	PSNR	MSSIM	VIF	C_R	MSE	PSNR	MSSIM	VIF	C_R	MSE	PSNR	MSSIM	VIF
Monkey	0.125	98.44	75.69	29.34	0.39564	0.46	98.44	77.20	29.27	0.48596	0.21	9 8 .4 4 9 6 8 8 9 3	80.21	29.09	0.40115	0.16	9 8 .4 4 9 6 8 8 9 3	78.77	29.18	0.38546	0.18
	0.25	96.88	55.64	30.69	0.6206	0.57	96.88	56.14	30.65	0.64028	0.36	9 8 8 9 3	65.80	29.95	0.58852	0.30	9 8 8 9 3	66.24	29.93	0.51891	0.34
	0.50	93.75	38.06	32.35	0.78925	0.70	93.75	49.76	31.17	0.75393	0.42	9 5 9 0 0 3	52.33	30.96	0.7271	0.46	9 7 5 9 0 6 3 8 7	53.73	30.84	0.66763	0.54
	0.75	90.63	27.38	33.80	0.86414	0.72	90.63	28.56	33.59	0.83579	0.60	9 6 3 8 7	42.29	31.89	0.80867	0.53	9 6 3 8 7	42.29	31.88	0.75731	0.71
	1	87.50	17.13	35.45	0.91204	0.72	87.50	24.39	34.28	0.87396	0.62	9 5 0 8 1	38.50	32.30	0.84716	0.53	9 5 0 8 1	38.92	32.25	0.79005	0.75
	1.5	81.25	6.41	41.05	0.96937	0.87	81.25	14.30	36.79	0.93073	0.79	9 2 5 7 5	16.79	35.95	0.92466	0.73	9 2 5 7 5	27.10	33.83	0.86549	0.89
Lena	2	75.00	4.48	42.69	0.98052	0.90	75.00	9.35	38.45	0.95288	0.80	9 0 0	9.31	38.61	0.95564	0.83	9 0 0	21.37	34.88	0.89257	0.92
	0.125	98.44	61.78	30.27	0.66676	0.61	98.44	74.58	29.41	0.70292	0.29	9 8 .4 4 9 6 8 8 9 3	72.30	29.56	0.6624	0.25	9 8 .4 4 9 6 8 8 9 3	58.38	29.48	0.66408	0.27
	0.25	96.88	26.05	34.01	0.83282	0.76	96.88	44.98	31.62	0.80321	0.46	9 6 8 8 9 3	45.68	31.54	0.78165	0.41	9 6 8 8 9 3	33.48	31.90	0.77311	0.50
	0.50	93.75	13.36	37.02	0.90236	0.79	93.75	18.28	35.58	0.87491	0.65	9 5 9 0 0	27.44	33.78	0.85925	0.57	9 7 5 9 0	20.39	35.10	0.86457	0.78
	0.75	90.63	9.56	38.51	0.922	0.88	90.63	12.52	37.23	0.89053	0.72	9 6 3 8 7	15.65	36.34	0.90069	0.74	9 6 3 8 7	16.49	36.04	0.88209	0.88
	1	87.50	6.92	39.93	0.93444	0.89	87.50	11.93	37.43	0.89952	0.76	9 5 0 8 1	13.08	37.05	0.9106	0.75	9 5 0 8 1	12.80	37.18	0.90554	0.91
	1.5	81.25	4.30	42.74	0.95284	0.89	81.25	7.92	39.20	0.9161	0.81	9 2 5 7 5	7.68	39.47	0.93354	0.83	9 2 5 7 5	8.83	38.82	0.92472	0.96
Concord aerial Image	2	75.00	2.27	45.44	0.96915	0.95	75.00	4.28	41.89	0.93131	0.87	9 0 0	4.92	41.34	0.95037	0.88	9 0 0	6.91	39.91	0.93751	0.98
	0.125	98.44	64.67	30.07	0.48212	0.65	98.44	92.80	28.46	0.41884	0.17	9 8 .4 4 9 6 8 8 9 3	74.41	28.56	0.46376	0.17	9 8 .4 4 9 6 8 8 9 3	85.17	28.83	0.33451	0.14
	0.25	96.88	37.16	32.44	0.72959	0.89	96.88	74.23	29.44	0.61637	0.33	9 6 8 8 9 3	53.43	28.99	0.66352	0.23	9 8 8 9 3	71.81	29.57	0.48655	0.30
	0.50	93.75	18.35	35.50	0.87817	0.96	93.75	48.72	31.29	0.76267	0.50	9 7 5 9 3	30.55	30.09	0.83292	0.43	9 7 5 9 3	57.79	30.51	0.66733	0.56
	0.75	90.63	10.43	37.95	0.92554	0.96	90.63	42.26	31.95	0.82157	0.53	9 0 0	17.44	30.84	0.89245	0.46	9 0 0	52.29	30.95	0.74509	0.62

1	87.50	6.85	39.77	0.95008	0.99	87.50	26.45	34.11	0.87334	0.67	6	3	8	7	6
1.5	81.25	0.56	51.13	0.99732	0.99	81.25	17.24	36.17	0.91867	0.72	5	0	8	1	5
2	75.00	0.44	52.35	0.99812	1.00	75.00	7.85	40.13	0.94971	0.84	2	5	7	5	0

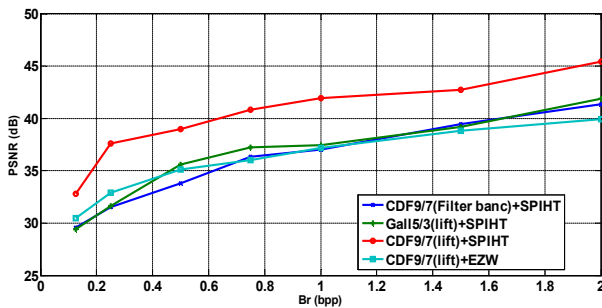


Figure. 9. 'Lena' image, PSNR variation using different methods

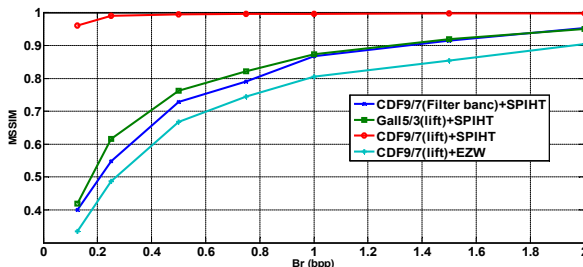


Figure. 10. 'Concord aerial' image, MSSIM variation using different methods

The comparison is made in terms of energy consumption and image quality for the four algorithms. First, the energy consumption measured by the compression ratio criterion (CR) indicated in Table 2, compression ratio (CR) is obtained by the same values of the same bit rate of four algorithms and better than the ones obtained in [25-27]. To judge by these four algorithms, we used another factor is the image quality, the latter is based on the criteria MSE, PSNR, MSSIM and VIF curves, which are shown in Figures 9, 10 and 11. By comparing the different values of MSE, PSNR, MSSIM and VIF; we notice on that, MSE of CDF9/7 (Lifting) + SPIHT algorithm is better than other algorithms, and even better than the results obtained in [26-28]. PSNR of CDF9/7(Lifting) + SPIHT algorithm give better results than other algorithms, and the results obtained in [2-3] [26-29], are more precise this clearly show the effectiveness of the CDF9/7 (Lifting) + SPIHT algorithm compressed in terms of image quality. The different results obtained after application of the algorithm on a different edge. These results are obtained with a bit rate compression

of 0.75 bpp. We note that CDF 9/7 (Lifting) + SPIHT is suitable for use in WMSN in terms of, power consumption and image quality.

8. Conclusion

This paper has discussed four compression techniques to WMSN with comparison between them and the factors affecting both techniques. Energy consumption and image quality are the most important indicators discussed for compression performance. Compression is considered an essential tool to facilitate the transmission of colour images. After several applications, we have shown that the biorthogonal wavelet compression CDF 9/7 based on a lifting scheme, coupled with the SPIHT coding gives better results compared to other compression techniques.

To develop our algorithm, we applied it on different types of colour images. We observed that for 0.75 bpp bit rate, the algorithm provides very high values for such images as MSE, PSNR, MSSIM and VIF, and it is more appropriate for this category of images. Thus, we conclude that the results obtained are very satisfactory in terms of compression ratio and quality of the compressed image.

ACKNOWLEDGEMENTS

The authors would like to be grateful to the Editor and anonymous reviewers for their invaluable comments and suggestions, which have improved the quality of the paper.

REFERENCES

- [1] H. ZainEldin, M A. Elhosseini, and H A. Ali , Image compression algorithms in wireless multimedia sensor networks: A survey, *Ain Shams Eng J*, Vol 6, No 2, pp. 481–490, 2015.
- [2] M.Tao , M.Hempel, P.Dongming, and H.Sharif, A survey of energy-efficient compression and communication techniques for multimedia in resource constrained systems, *Communications Surveys & Tutorials IEEE*, Vol 15, No 3 ,pp. 963–72,2013.
- [3] M. Nasri, A. Helali, H. Sghaier, H. Maaref, Adaptive image compression technique for wireless sensor networks, *Computers & Electrical Engineering*, Vol 37, No 5, pp.798–810, 2011.
- [4] O. Ghorbel, W. Ayedi, M.W. Jmal, and M. Abid, Image compression in WSN: performance analysis , *Communication technology (ICCT), IEEE 14th international conference*, pp. 1363–8, 2012.
- [5] W. Chew Li, A. Li-Minn, and P.Seng Kah, Survey of image compression algorithms in wireless sensor networks, *IEEE*

information technology. ITSim 2008. *International symposium*, Vol 4, 2008, pp. 1–9, 2008.

[6] M. Beladgham, A. Bessaïd, A. Moulay-Lakhdar, M. BenAissa, and A. Bassou, MRI IMAGE COMPRESSION USING BIORTHOGONAL CDF WAVELET BASED ON LIFTING SCHEME AND SPIHT CODING, *Quatrième Conférence Internationale sur le Génie Electrique CIGE'10*, Université de Bechar Algérie, pp. 225–232, 2010.

[7] M. Beladgham, A. Bessaïd, A. Moulay-Lakhdar, and A. Taleb-Ahmed, Improving Quality of Medical Image Compression Using Biorthogonal CDF Wavelet Based on Lifting Scheme and SPIHT Coding, *SERBIAN JOURNAL OF ELECTRICAL ENGINEERING*, Vol 8, No 2, pp. 163–179, 2011.

[8] A. Said, and W.A. Pearlman, An Image Multiresolution Representation for Lossless and Lossy Compression, *IEEE Transactions on Image Processing*, Vol 5, N° 9, pp. 1303 – 1310, 1996.

[9] J.D. Zandi Allen, E.L. Schwartz, and M. Boliek, CREW Compression with Reversible Embedded Wavelets, *Data Compression Conference*, Snowbird, USA, pp. 212 – 221, March 1995.

[10] A. Said, and W.A. Pearlman, A New Fast and Efficient Image Codec based on Set Partitioning in Hierarchical Trees, *IEEE Transaction on Circuits and Systems for Video Technology*, Vol 6, No 3, pp. 243 – 250, 1996.

[11] J.D. Villasenor, B. Belzer, and J. Liao, Wavelet Filter Evaluation for Image Compression, *IEEE Transactions on Image Processing*, Vol 4, No 8, pp.1053 – 1060, 1995.

[12] G. Pau, Advanced Wavelets and Space-time Decompositions: *Application to Video Coding Scalable*, Phd thesis, National School of Telecommunications, Paris, 2006.

[13] A. Savakis, and R. Carbone, Discrete Wavelet Transform Core for Image Processing Applications, Real-time Imaging IX, *SPIE-IS&T Electronic Imaging*, San Jose, CA, USA, SPIE Vol 5671, , pp. 142 – 151, Jan 2005.

[14] P.S.A. Kumar, *Implementation of Image Compression Algorithm using Verilog with Area, Power and Timing Constraints*, MasterThesis, National Institute of Technology, Rourkela, India, 2009.

[15] M. Benaïssa, A. Bassou, M. Beladgham, A. Taleb-Ahmed, and A. Moulay-Lakhdar, Application of 16-State TCM-UGM and TCM for Improving the Quality of Compressed Color Image Transmission, *International Journal of Image, Graphics and Signal Processing*, Vol 6, No 10, pp.10-17, 2014

[16] W.S. Geisler, and M.S. Banks, Visual performance, in *Handbook of Optics* (M.Bass, ed.), McGraw-Hill, 1995.

[17] A.B. Watson, and L. Kreslak, Measurement of visual impairment scales for digital video, in *Human Vision, Visual Processing, and Digital Display*, Proc. SPIE, Vol 4299, 2001.

[18] Z. Wang, A.C. Bovik, H.R. Sheikh, and E.P. Simoncelli, Image quality assessment: From error visibility to structural similarity, *IEEE Transactions on Image Processing*, Vol 13, No 4, pp. 600-612, 2004.

[19] Z. Wang, and A.C. Bovik, A universal image quality index, *IEEE Signal Processing Letters*, Vol 9, No 3, pp. 81–84, 2002.

[20] K. SESHADRINATHAN, H.R.SHEIKH, , Z. WANG, and A. C.BOVIK, Structural and Information Theoretic Approaches to Image Quality Assessment, *Multi-Sensor image fusion and ITS Application*, pp 1-39, 2005.

[21] E. Dumić, S. Grgić, and M. Grhić, New image-quality measure based on wavelets, *Journal of Electronic Imaging*, Vol 19, No 1, pp. 011018 1-19,2010.

[22] A.K. Moorthy, Z. Wang, and A.C.Bovik, Visual Perception and Quality assessment, *Chapter19 in Optical and digital image processing*, Wiley, 2010.

[23] Z. WANG, and Q. LI, Information Content Weighting for Perceptual Image Quality Assessment, *IEEE Transactions on Image Processing*, Vol 20, No 5, pp. 1185-1198, 2011.

[24] Z. Xiong, K. Ramchandran, and M.T.Orchard, Space-frequency Quantization for Wavelet Image Coding, *IEEE Transaction on Image Processing*, Vol 6, No 5, pp. 677 – 693,1997.

[25] L.Chih-Chung, C.Chi-Cheng, C.Chien-Wen, and C. Ray-I, A novel data compression method using improved JPEG-LS in wireless sensor networks, *IEEE Conference Publications Advanced Communication Technology (ICACT)*, 2010 The 12th International Conference on, Vol 1, pp. 346 – 351, 7-10 Feb 2010.

[26] A. Loganathan, R. Hemalatha, and Dr. S. Radha, Comparison of encoding techniques for transmission of image data obtained using Compressed Sensing in Wireless Sensor Networks, *IEEE Conference Publications Recent Trends in Information Technology (ICRTIT)*, International Conference on, pp. 696 – 701, Chennai, July 2013.

[27] B. Amol, A. Shweta, and C. Amruta, Performance Evaluation of High Quality Image Compression Techniques, *IEEE Conference Publications Advances in Computing, Communications and Informatics (ICACCI)*, 2014 International Conference on, , pp. 1986 – 1990, New Delhi,Sept 2014.

[28] S.P. Raja1, and Dr. A. Suruliandi, Performance Evaluation on EZW & WDR Image Compression Techniques, *IEEE Conference Publications Communication Control and Computing Technologies (ICCCCT)*, 2010 IEEE International Conference , pp. 661 – 664, Ramanathapuram, Oct 2010.

[29] O. Ghorbel, I. Jabri, , W. Ayedi, and M. Abid, Experimental study of compressed images transmission through WSN, *IEEE Conference Publications Microelectronics (ICM), International Conference on*, pp. 1-6, Hammamet, Dec 2011.



Haouari BENLABBES; was born in Bechar, Algeria. He received the dipl. El.-Ing.from the university of Bechar, Algeria, and then a Master in Informatics from the university of Bechar, Algeria. Since December 2014, he enrolled in doctoral at the university of Bechar. His research interests are WMSN, WSN, Image and video processing.



Khelifa Benahmed, has done his research for Ph.D. degree in the field of sensor networks wireless at the school of computing and mathematical sciences at Liverpool John mores university, UK. He has 26 years of experience in education and research at the University Tahri Mohamed Bechar, Algeria. Khelifa has also several international publications in the fields: wireless sensor networks, security, surveillance, smart grid, Internet of things, and smart irrigation. Khelifa holds Engineer, Magister degrees and PhD in Computer sciences in University of Oran Algeria.



Mohammed BELADGHAM was born in Tlemcen, Algeria. He received the dipl. El.-Ing.from the university of Tlemcen, Algeria, and then a Master in signals and systems from the university of Tlemcen, Algeria. Since December 2012, he graduated PhD Es Sciences at the University of Tlemcen. His research interests are Image processing, Medical image compression, wavelets transform and optimal encoder.